



## Sedimentation properties and modeling of dredged soil

Min-Sun Lee & Kazuhiro Oda

To cite this article: Min-Sun Lee & Kazuhiro Oda (2018): Sedimentation properties and modeling of dredged soil, Marine Georesources & Geotechnology

To link to this article: <https://doi.org/10.1080/1064119X.2017.1420714>



Published online: 16 Jan 2018.



---

Submit your article to this journal [↗](#)



---

View related articles [↗](#)



---

View Crossmark data [↗](#)

---



## Sedimentation properties and modeling of dredged soil

Min-Sun Lee<sup>a</sup>  and Kazuhiro Oda<sup>b</sup>

<sup>a</sup>Disaster Prevention System & Analysis, Hydro-soft Technology Institute, Japan; <sup>b</sup>Department of Civil Engineering, Graduate School of Engineering, Osaka University, Osaka, Japan

### ABSTRACT

When dredged soil containing coarse soil is used for the construction of reclaimed ground that is in contact with the surface of seawater, there is a high possibility of the generation of nonuniformly reclaimed ground due to the segregation of fine-grained soil from coarse-grained soil. It is difficult to assume uniform properties of reclaimed ground because the properties are defined and formed by the spontaneously segregating sedimentation. Estimation of the soil's volume change lacks accuracy if the properties of the reclaimed ground are assumed to be always uniform. Therefore, for pump-dredged reclamation, a predictive study and various experiments are required to estimate the physics and properties of the dredged soil sedimentation. Accordingly, this study demonstrates a modeling test to understand the characteristics of the sedimentary ground using the changing ratio of fraction of the sample passing through a 75- $\mu\text{m}$  sieve. The effect of particle arrangement on hindered settling properties, sedimentation properties, the distribution of water content of sedimentary ground, and physical properties can be determined by the modeling test. The study also suggests the calculation method for the travel distance of the outlet and the volume of input soil based on the experimental results.

### ARTICLE HISTORY

Received 5 September 2017  
Accepted 18 December 2017

### KEYWORDS

Dredged soil; modeling test; reclaimed ground; segregating sedimentation; soil properties

### Introduction

Methods for the construction of reclaimed ground are generally classified into two main types: pump dredging reclamation and grab bucket dredging reclamation. The pump dredging method transfers soil and seawater to the construction site with a suction transfer pipe using a pump dredger (Masaaki, Masaaki, and Akira 2001). This method is financially efficient, but it is not effective for construction if soil needs to be transferred a long distance. In the grab-bucket dredging method, soil and water from the ocean floor are collected and transferred by a carrying vessel to the construction site. The method is ideal for construction when soil needs to be transferred over a long distance and when the collected soil has low water content. The grab-bucket method is also recommended if installation of a pump dredger is not possible. However, the grab-bucket dredging method pollutes the soil and water at the ocean floor at the moment of collection and appropriate countermeasures are required for this damage. The grab-bucket method has less construction efficiency compared with the pump dredging method. For these reasons, the pump dredging reclamation method is used widely for large-scale reclamation construction (Chu, Bo, and Arulrajah 2009). For pump dredging reclamation, the sedimentation, self-weight consolidation properties, and other conditions are varied to maintain the slurry state of the soil (Imai 1981). For example, the location of sand discharge pipe, input velocity, area of reclaimed ground, height of the reclamation, diameter of the dredged coarse soil, and initial water content are all varied.

The process of soil sedimentation in general consists of three stages. (1) In the flocculation stage, no settling takes place, but flocculation yields flocs. (2) In the settling stage, the flocs gradually settle, forming a layer of sediment that undergoes consolidation and reduction of water content. (3) In the consolidation stage, all of the sediment thus formed undergoes self-weight consolidation and finally approaches an equilibrium state (Lee and Oda 2013b). The properties and conditions of the reclaimed ground are dependent on and affected by the sedimentation and settlement processes (Lee and Oda 2015). In particular, when ground is being reclaimed in contact with the surface of seawater, the dredged soil is collected by a transfer pump. Additionally, the properties of the reclaimed ground are affected by the soil and the pipe distance to the outlet. For this reason, the properties of the reclaimed ground may not always be uniform. Without consideration of the varying distance to the outlet and the effect on particle arrangement, estimation of the volume of the sedimentation may be either overestimated or underestimated. In addition, the differential settlement may cause problems for the construction (Lee and Oda 2013a). At present, there are no studies defining the effect of pipe distance to the outlet on sedimentation properties when performing reclamation in contact with the surface of seawater. The goal of this research is to suggest a sedimentation modeling test to estimate the sedimentation properties for the case in which land reclamation is performed in contact with seawater. Therefore, this study aims to define the mechanics of the

sediment and the properties of reclaimed ground with dredged soil containing coarse soil. The study also aims to suggest a construction method for reclamation by dredging with consideration of the effect of particle arrangement by segregating coarse soil and settling fine soil.

**Sedimentation modeling test**

**Physical properties of the dredged soil**

Table 1 shows the physical properties of the sample soil, and Figure 1 shows the grain size distribution curves of the

**Table 1.** Physical properties of the dredged soil used in this study.

Sample no.	1	2
Plasticity index		NP
Specific gravity		2.695
Amount passing through 75- $\mu$ m sieve (%)	20	45
Coefficient of uniformity	5	12
Coefficient of curvature	1.01	1.33
USCS		SM
Note	Adjust the grain size	

samples being tested. The sample consists of dredged soil that was collected from the construction site for this experiment. The sample particles were filtered and adjusted by the percentage passing through a 75- $\mu$ m sieve. Sample 1 has 20% of material passing through the 75- $\mu$ m sieve, and sample 2 has 45%. Sample 1 has a coefficient of uniformity of 5 and a coefficient of curvature of 1.01. Sample 2 has a coefficient of uniformity of 12 and a coefficient of curvature of 1.33. In other words, sample 2 has a better grain size distribution than sample 1. According to the Unified Soil Classification System, samples 1 and 2 are classified as silty sand, SM.

**Experimental and measurement apparatus**

Figure 2 shows the apparatus used for the sedimentation modeling tests. The apparatus was installed for modeling and demonstrating the possible sedimentation conditions after input of slurry at the construction site. The dimensions of the pond were 70  $\times$  300  $\times$  70 cm. The sides of the pond were constructed with transparent acrylic to measure the soil’s sedimentation height and elevation of the interface. In addition, a container was installed to maintain the slurry state of the input soil. In the experiment, the slurry sample in the container is transferred to and poured into the pond. To avoid sedimentation of the slurry sample before input, a mixer and a hose connected to an air compressor were installed in the container. To transfer the slurry, an underwater pump and a transfer hose with a diameter of 1.3 cm were installed. Figure 3 shows the installation locations of the measurement apparatus. To measure the dynamical properties of the sedimentation, piezometers and earth pressure gauges were installed. In total, three piezometers were installed at locations P1, P2, and P3, and two earth pressure gauges were installed at locations E1 and E2. A scale was also installed at each location, at distances of 40 cm (S1), 160 cm (S2), and 280 cm (S3) away

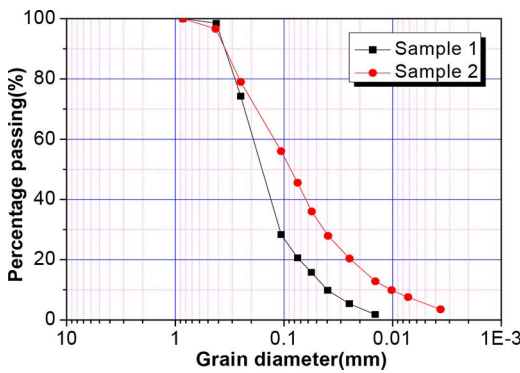


**Figure 1.** Grain size distribution of dredged soil.

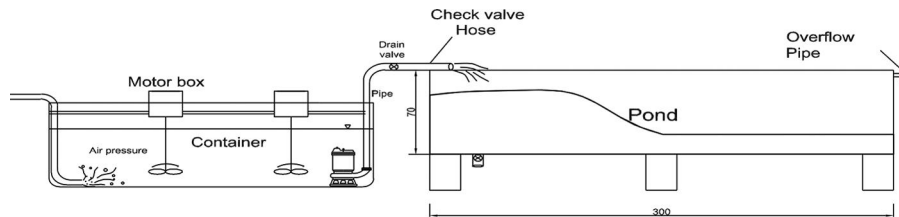


**Figure 2.** Apparatus used for sedimentation modeling tests.

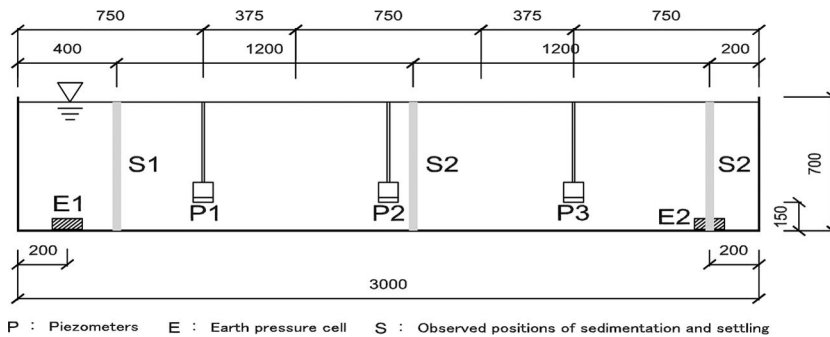


**Figure 3.** Installation locations of measurement apparatus.

**Table 2.** Experimental conditions.

	Water content (%)	Input velocity (m <sup>3</sup> /min)	Volume of input (m <sup>3</sup> )	Elapsed time for each step (min)	Total steps	Sample no.
Case 1	700	0.59	0.63	200	4	1
Case 2	700	0.59	0.63	200	4	2

**Table 3.** Time taken for each step.

Step	Input	Observation	Time (min)		
			Removal of surface water	Lapse	Cumulative sum
1	2	193	27	222	222
2	2	145	51	198	420
3	2	108	70	180	600
4	2	145	53	200	800

from the outlet, to measure the sedimentation and settling heights.

### Experiment method

Table 2 shows the experimental conditions. First, we prepared the slurry sample with a water content of 700% in the container using seawater. The volume of the input soil in the step 1 was 0.63 m<sup>3</sup>. The mixer and water pressure were used before inserting the sample to prevent sedimentation. The input velocity was the same as the input velocity of the pump, 0.59 m<sup>3</sup>/min. After the input, the earth pressure and pore water pressure were measured using the measuring apparatus. The sedimentation height and elevation of the interface were also measured. When the sedimentation and settlement had completed, soil was poured repeatedly using the same method to demonstrate the phased input of dredged soil. In step 1, it is important to note that the slurry sample is being poured into the container with water to demonstrate the construction of the foundation of the reclaimed ground. In step 2, the surface water was removed before input to demonstrate the construction of reclaimed ground that is in contact with the surface of seawater. We finally demonstrated all 4 steps of the phased input. For the case 1, the experiment was performed with sample 1; for case 2, it was performed with sample 2. Table 3 shows the time taken for each step. The average elapsed time for each step was 200 min, and the average observation time was 148 min. The total cumulative time of the experiment was 800 min.

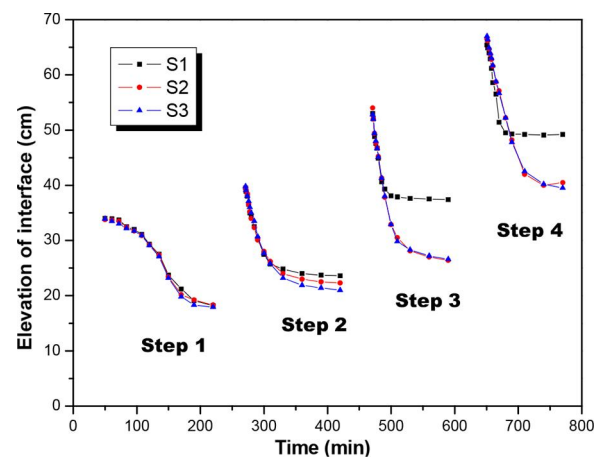
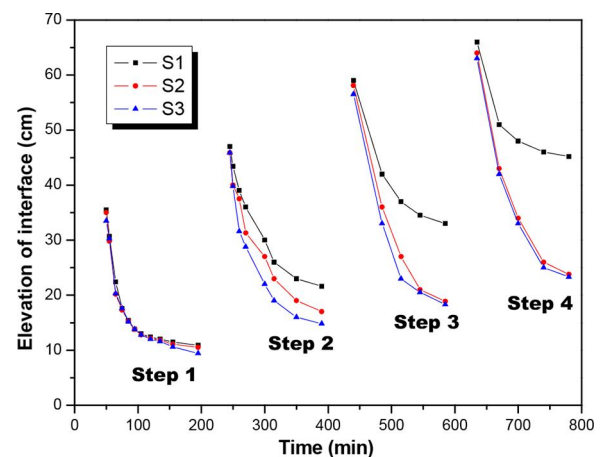
### Sedimentation modeling experimental data

#### Relationship between elevation of interface and time

Figure 4 shows the relationship between the elevation of the interface and time for case 1, and Figure 5 shows this relationship for case 2. In the figures, S1, S2, and S3 represent the measured elevations of the interface (according to Figure 3). The elevation of the interface at S1 is the elevation closest to the outlet, and it has higher elevation of the interface than S2 or S3. In other words, a larger volume of poured slurry sample is deposited near the outlet. The reason for this difference is that coarse soil is deposited near the outlet as it is being poured, but fine soil remains suspended and is deposited far

from the outlet after being discharged horizontally by the pressure of the pump. Therefore, lower elevations of the sedimentation are observed at S2 and S3, and the elevation generally decreases with distance from the outlet. On the other hand, the relationship between elevation of the interface and time for S2 and S3 is nearly the same. Therefore, soil at S2 and S3 has similar sedimentation properties because the soil particle size does not significantly differ between these two points.

Figure 6, which compares the experimental data of step 3, shows the effect of particle arrangement on the relationship between elevation of the interface and time. It can be estimated that the typical settling stage of case 1 is 14 min and that the settling stage of case 2 is 45 min. After 14 and 45 min, respectively, for each case, the time is regarded as the consolidation stage (Imai 1980). The gradient of case 2 is more gradual than the gradient of case 1 because case 2 has more fine soil per time change of the elevation of the interface. In

**Figure 4.** Relationship between elevation of interface and time (case 1).**Figure 5.** Relationship between elevation of interface and time (case 2).

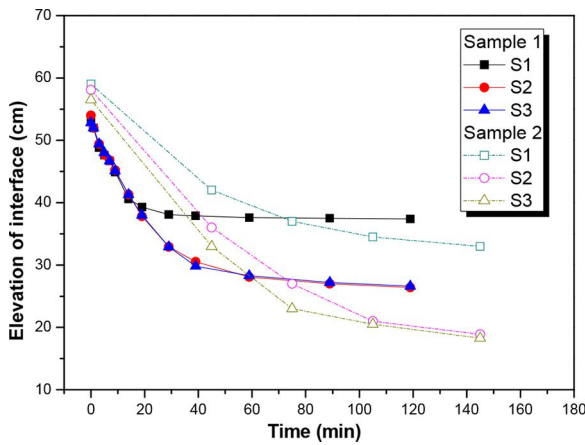


Figure 6. Effect of particle arrangement on relationship between elevation of interface and time (step 3).

other words, the sedimentation velocity is faster if there is more coarse soil in the slurry. Because there is more coarse soil in case 1 than in case 2, the sedimentation velocity of case 1 is observed to be faster. It is also observed that heavier self-weight consolidation occurs in case 2 than in case 1, in which self-weight consolidation is completed in the consolidation stage. In other words, the elevation of the interface of case 2 is lower. The volume of the self-weight consolidation in case 1 is smaller than that in case 2. The reason for this is that the sample, used in case 1 has more coarse soil than the sample used in case 2, resulting in the smaller volume of the self-weight consolidation.

**Sedimentation properties**

Figure 7 shows the horizontal distribution of the interface elevation of case 1, and Figure 8 shows the horizontal distribution of the interface elevation of case 2. Here, the elevations are the final interface elevation of each step. The interface elevation gradually increases between steps (e.g., step 2 has a higher interface elevation than step 1). After step 2, the interface elevation is at its highest at 50–75 cm away from the outlet. The interface elevation decreases between the regions of 50–75 cm from the outlet and 160 cm from the

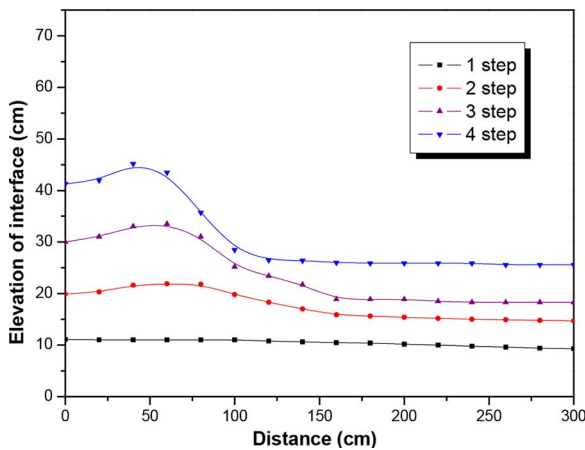


Figure 7. Horizontal distribution of interface elevation (case 1).

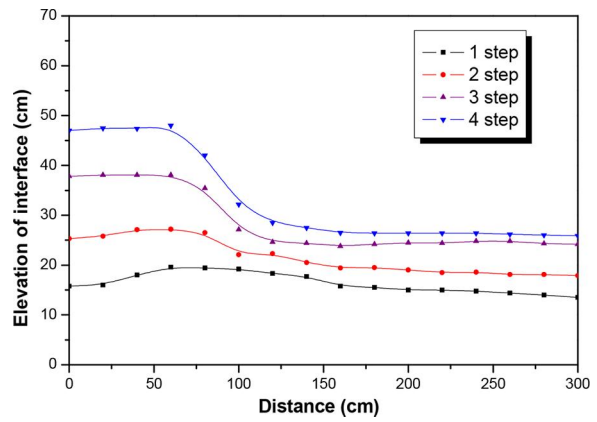


Figure 8. Horizontal distribution of interface elevation (case 2).

outlet. The interface elevation then distributes at a constant height between the regions of 160 cm from the outlet and 300 cm from the outlet. The horizontal location changes of the interface elevation can be explained by the following reason. In the experiment, the horizontal discharge of soil occurs in the region of 50–75 cm away from the outlet. At the moment of discharge, the coarse soil in the dredged soil is deposited immediately at that location. Therefore, the coarse soil is deposited around the location of 50–75 cm from the outlet. Because the test sample consists of more coarse soil than fine soil, there is a larger amount of coarse soil deposited nearer the outlet than fine soil deposited far from the outlet after horizontal suspension. Thus, higher interface elevation is measured at the region 50–75 cm away from the outlet. In the area between 160 and 300 cm from the outlet, the fine soil, including some coarse soil, moves horizontally by the action of the pressure pump. Some dredged soil from the previous step gets swept away with the fine soil, and segregating sedimentation of coarse soil is observed from this time. However, the fine soil experiences hindered settlement at the moment. Therefore, the interface elevation appears to be constant. The area 75–160 cm from the outlet is the transition region, a change from the sedimentation region of the coarse soil to the sedimentation region of the fine soil. Figure 9 shows the horizontal distribution of interface elevation for four cases

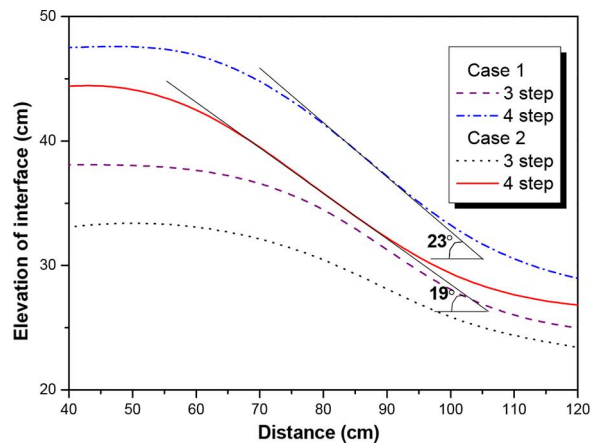


Figure 9. Horizontal distribution of interface elevation (distance range 40–120 cm; cases 1–4).

**Table 4.** Angle of slope.

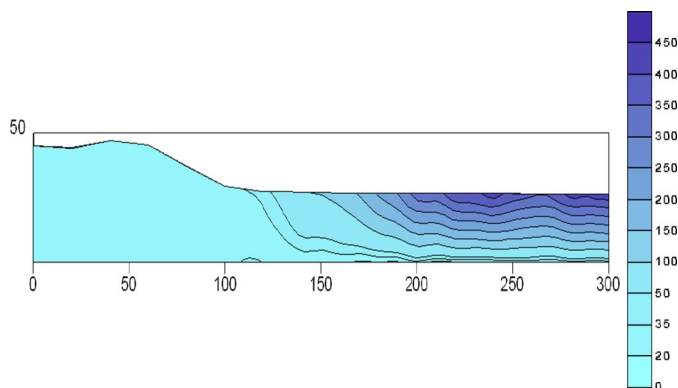
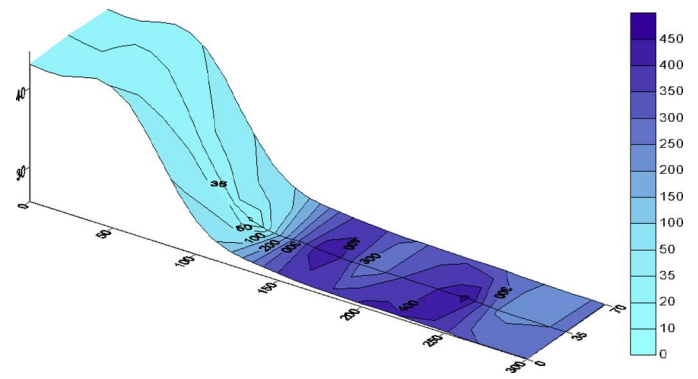
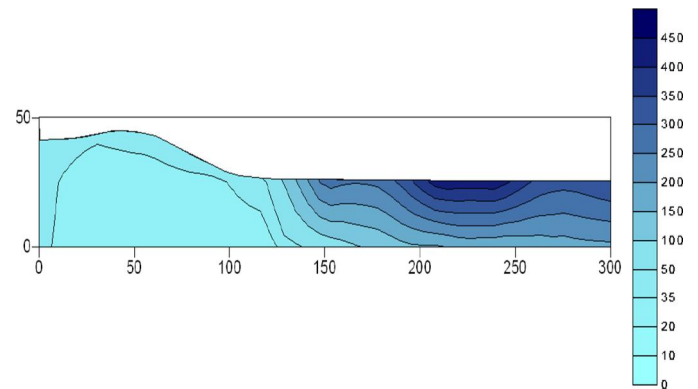
Classification	Angle of slope (°)
Clay (dry)	20–40
Clay (under water)	15
Gravel (dry)	30–45
Gravel (natural)	25–30
Sand (dry)	34
Sand (saturated)	15–30
Sand (wet)	45

(1–4). It is normally seen that when a slurry sample is poured in a site, it is formed like a cone shape. The sedimentation region of the coarse soil orients itself and a certain angle of deposition repose. This angle is affected by the type of soil and the soil internal friction angle (Ghazavi, Hosseini, and Mollanouri 2008). The larger the gradient angle means increasing particle size or increasing friction coefficient.

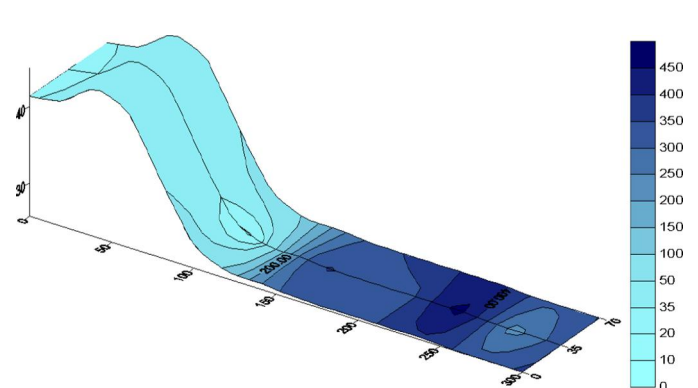
After the completion of the experiment, the maximum gradient of the interface elevation was measured from the horizontal distribution of the interface elevation. As a result, case 1 has a gradient angle of 23°, and case 2 has a gradient angle of 19°. The angle of the slope of case 1 is larger than that of case 2. Table 4 shows the angles of slope that are stable, i.e., the soil does not collapse by itself (Hough 1957). The angle for soil under water is 15°, and the angle for saturated sand is 15–30°. The angles of the slopes of cases 1 and 2 are located within the range of the angle of slope for saturated sand. Therefore, it is estimated that the angles of the slopes of cases 1 and 2 are determined by the amount of coarse soil included. On the other hand, the angle of the slope of case 1 is larger than the angle of case 2 because sample 1 has more coarse soil than sample 2.

#### Distribution of water content of sedimentary layer

Figure 10 shows the distribution of the cross-sectional water content in the pond after the case 1 experiment was completed, and Figure 11 shows the distribution of the surface water content after the case 1 experiment was completed. Figures 12 and 13 show these distributions, respectively, for the case 2 experiment. The water content was measured after removing the supernatant when the experiment had been completed. The cross section of the case 1 pond was estimated by collecting samples from 115 places. On the surface, samples

**Figure 10.** Distribution of cross-sectional water content (case 1).**Figure 11.** Distribution of surface water content (case 1).**Figure 12.** Distribution of cross-sectional water content (case 2).

were taken from 48 places and the water content was calculated on the basis of the data. For case 2, 56 samples were taken from the cross section of the pond, and the water content was calculated on the basis of these data. On the surface, 33 samples were taken to calculate the water content. As a result, wide ranges of water content, varying from 5 to 500%, were estimated. The distribution of the pond's cross-sectional water content was classified into three sections (stages) based on its properties. Stage I represents the distance from the outlet to 100 cm, stage II is the distance from 100 to 150 cm, and stage III is the distance from 150 to 300 cm. In stage I, the water content is 20–50% (Figures 10–12). In this stage, coarse soil with a small amount of fine soil is deposited; therefore, the water content is low. On the other hand, the

**Figure 13.** Distribution of surface water content (case 2).

water content in stage III is 100–500%. In this stage, fine soil with a small amount of coarse soil is deposited. At the same height, the water content is constant irrespective of the distance from the outlet. In addition, the water content increases with proximity to the surface. The reason for this observation is that previously deposited sediment is mixed and disturbed by subsequently transferred soil. After this occurs, hindered settling takes place. Therefore, the water content increases closer to the surface. In stage II, the water content is 30–200%. This stage is the transition region. The water content distribution on the surface in stage I is 20–40%, which is the lowest of the three stages. In stage II, the water content is 40–300%. In stage III, it is 300–500%. The distribution of the water content in stage I is caused by the sedimentation of coarse soil with some fine soil. Therefore, it is estimable that the water content of the surface is lower. On the other hand, fine-soil hindered settling is dominantly observed in stage III. Therefore, the water content on the surface increases rapidly. The transition region is stage II, so its surface water content ranges widely.

#### Sedimentary layer distribution of passing 75- $\mu\text{m}$ sieve

Figure 14 shows the pond cross-sectional distribution of soil passing through the 75- $\mu\text{m}$  sieve after the case 1 experiment was completed, and Figure 15 shows the distribution of the surface passing through the 75- $\mu\text{m}$  sieve after the case 1

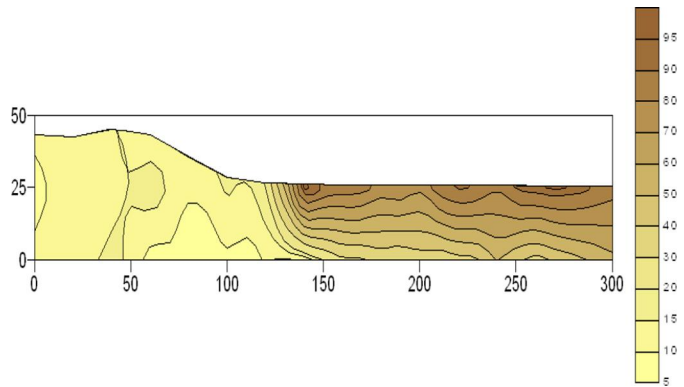


Figure 14. Cross-sectional distribution of soil passing the 75- $\mu\text{m}$  sieve (case 1).

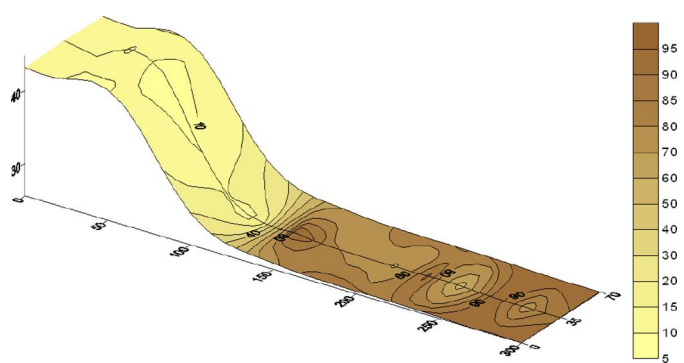


Figure 15. Cross-sectional distribution of surface passing the 75- $\mu\text{m}$  sieve (case 1).

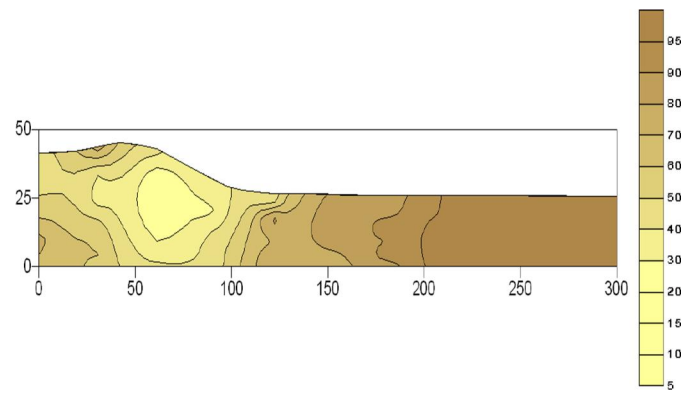


Figure 16. Cross-sectional distribution of soil passing the 75- $\mu\text{m}$  sieve (case 2).

experiment was completed. Figures 16 and 17 show the distributions after the case 2 experiment was completed. The amount of soil passing the 75- $\mu\text{m}$  sieve was measured after removing the supernatant after the experiment had been completed. The cross-sectional distribution of the case 1 pond was estimated by collecting samples from 99 places. On the surface, samples were taken from 42 places. The percentage of soil passing the 75- $\mu\text{m}$  sieve was then calculated on the basis of the resulting data. For case 2, 56 samples were taken from the cross section of the pond and 28 samples were taken from the surface. The distribution of the pond's cross-sectional water content was again classified into 3 sections based on their properties: stage I, from the outlet to 100 cm; stage II, from 100 to 150 cm; and stage III, from 150 to 300 cm. In stage I, the sedimentation consists of soil with less than 50% passing through the 75- $\mu\text{m}$  sieve. Therefore, this stage represents mainly settling of coarse soil. However, in stage III, sedimentation occurs with soil having more than 50% that can pass the 75- $\mu\text{m}$  sieve. This stage is mainly settling of fine soil. In stage I of case I, the sedimentation has less than 50% of soil that can pass the 75- $\mu\text{m}$  sieve. In case 2, the amount of soil passing the 75- $\mu\text{m}$  sieve is higher than that in case 1. In particular, some areas have more than 50% passing the 75- $\mu\text{m}$  sieve in stage I. Case 2 has more fine soil in the dredged soil than case 1 because the sample used in case 2 has more fine soil than the sample used in case 1. This means that the percentage passing the 75- $\mu\text{m}$  sieve increases for case 2 compared to case 1. On the other hand, in case 1, stage III, increasing passage through

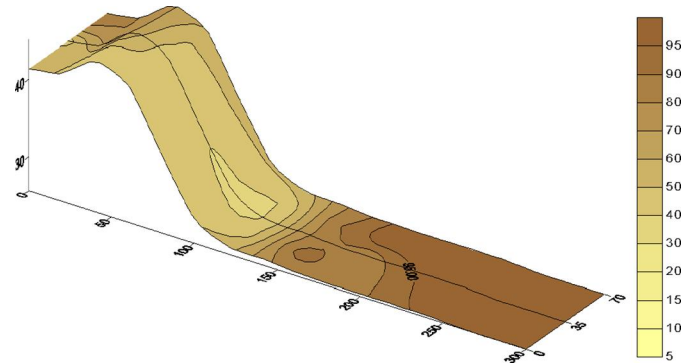


Figure 17. Cross-sectional distribution of surface passing the 75- $\mu\text{m}$  sieve (case 2).

the 75- $\mu\text{m}$  sieve is observed as the dredged soil gets closer to the surface. However, in case 2, the rate of passage through the 75- $\mu\text{m}$  sieve is constant; the value does not change when the amount passing the 75- $\mu\text{m}$  sieve is 80–100%. The reason for this observation is that previously deposited sediment is mixed and disturbed by subsequently transferred soil. After that, hindered settling takes place. Therefore, the amount passing the 75- $\mu\text{m}$  sieve increases with proximity to the surface. As in case 1, the previously deposited dredged soil in case 2 is mixed and disturbed by transferred soil at the moment of input. However, because there is a lesser amount of coarse soil included, the swept away soil in stage III is mostly fine soil. Therefore, the mixed and disturbed dredged soil is fine soil. It is estimated that the fine soil settles in layers, as suggested by the distribution of water content. However, the particles smaller than 75  $\mu\text{m}$  are impossible to classify due to the limitation of the sieve test. In stage II, the amount passing the 75- $\mu\text{m}$  sieve is 10–90% in case 1 and 40–80% in case 2. This stage is the transition region for both cases. On the surface, in stage I, the amount passing the 75- $\mu\text{m}$  sieve in case 1 is less than 20%, but the amount passing the 75- $\mu\text{m}$  sieve in case 2 is 40–80%. Case 2 has higher amounts of sediment passing the 75- $\mu\text{m}$  sieve than case 1 on the surface. This is affected by the suspending and settling of soil on the surface. In addition, if there are higher amounts of fine soil, more suspended and settling soil is observed. Therefore, case 2, with the sample with more fine soil, shows higher amounts of passage through the 75- $\mu\text{m}$  sieve on the surface. In stage III, the amount passing the 75- $\mu\text{m}$  sieve in case 1 is less than 80%, but in case 2, the amount passing the 75- $\mu\text{m}$  sieve is more than 80%. In stage II, the amount passing the 75- $\mu\text{m}$  sieve is 20–90% in case 1 and 40–90% in case 2. This stage represents the transition region for both cases.

Figure 18 shows the percentage of the area occupied by fine and coarse soil in each stage. Here, fine and coarse soil are classified according to the Unified Soil Classification System: fine soil has more than 50% of sediment passing the 75- $\mu\text{m}$  sieve and coarse soil has less than 50% passing the 75- $\mu\text{m}$  sieve. According to the Unified Soil Classification System, samples 1 and 2 both consist of coarse soil. After completion of the experiment, case 1 had 46.4% occupation by area of fine soil. Case 2 had 93.0% occupation by fine soil. When the

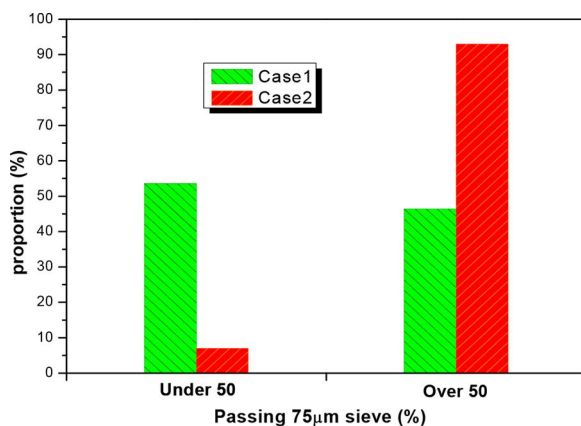


Figure 18. Percentage of area occupied by fine and coarse soil.

reclamation is processed with a sample with 20% passing the 75- $\mu\text{m}$  sieve, as in case 1, the percentage of occupational area of fine soil is approximately 50%. As shown in case 2, the reclaimed ground is dominated by fine soil when the initial soil had 45% passing the 75- $\mu\text{m}$  sieve. Therefore, the properties of the reclaimed ground and dredged ground are estimated differently according to the amount of coarse soil in the dredged soil. In other words, the area of fine soil occupation is increased in dredged soil that has a dominant amount of coarse soil. Figure 19 shows the relationship between the amount passing the 75- $\mu\text{m}$  sieve and water content. As shown in the figure, the water content increases as the amount of sediment passing the 75- $\mu\text{m}$  sieve increases. When the passing amount reaches 80%, the water content increases linearly within the range of 5–60%. When the amount passing the 75- $\mu\text{m}$  sieve increases from 80 to 85%, the water content increases rapidly from 60 to 100%. This relationship is reinterpreted as the following equation:

$$w = \frac{\ln(95.65 - p) - \ln 216.93}{\ln 0.96}, \quad (1)$$

where  $p$  is the amount passing the 75- $\mu\text{m}$  sieve and  $w$  is the water content.

### Vane shear strength properties

Figure 20 shows the pond distribution of cross-sectional vane strength after the case 1 experiment was completed. The distribution of the pond cross-sectional vane shear strength is also classified into three sections based on its properties. In stage I, the vane shear strength is 0.3–1.2 kPa. In stage II, the vane shear strength is 0.0–0.3 kPa, and in the stage III, it is 0.0 kPa at all positions. Because of the sedimentation of coarse soil with some fine soil in stage I, the speed of self-weight consolidation is faster. In this stage, the self-weight consolidation is almost completed. In addition, the vane shear strength is produced by low water content. In stage III, the speed of self-weight consolidation is slow because the fine soil has hindered settling. In this stage, self-weight consolidation is not yet complete. In addition, due to the high-water content, the effective stress is not yet observed. The transition region is stage II, in which vane shear strength decreases with

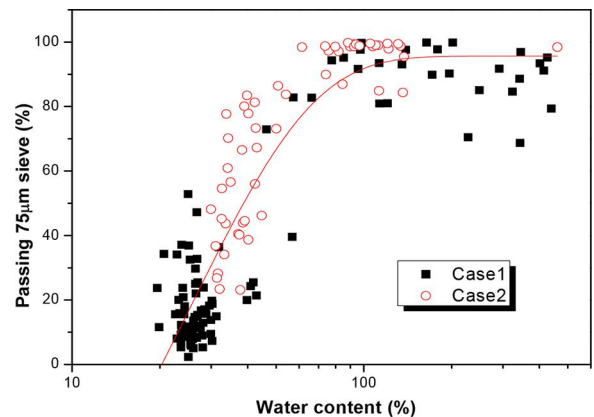


Figure 19. Relationship between amount passing 75- $\mu\text{m}$  sieve and water content.



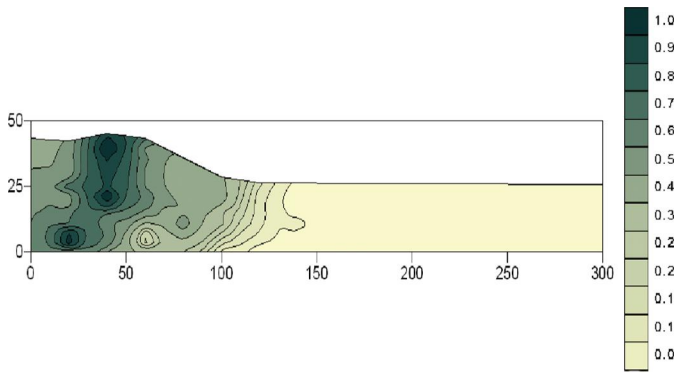


Figure 20. Cross-sectional distribution of vane shear strength (case 1).

distance from the outlet. From this, the stage of the process of self-weight consolidation can be estimated from the vane shear strength. Vane shear strength is observed in stage I; therefore, it is in the consolidation stage due to self-weight consolidation. However, vane shear strength is not revealed in stage III, so it is estimated that the self-weight consolidation process is not yet completed. Figure 21 shows the relationship between vane shear strength and water content for case 1. In the figure, the log of vane shear strength is used. As shown in the figure, the vane shear strength is equal to 0.01–1.2 kPa when the water content is 15–35%. However, the vane shear strength is 0.0 kPa when the water content is more than 35%. In other words, self-weight consolidation is completed when the water content is more than 35%, and that is why the vane shear strength is equal to 0.0 kPa. As shown in the figure, the vane shear strength increases as water content decreases within the water content range of 15–35%.

Figure 22 shows the relationship between the amount passing the 75- $\mu\text{m}$  sieve and vane shear strength for case 1. In the figure, the logarithm of vane shear strength is used. When the amount passing the 75- $\mu\text{m}$  sieve is 0–40%, the vane shear strength is 0.01–1.2 kPa. However, when it exceeds 40%, the vane shear strength is equal to 0.0 kPa. In other words, self-weight consolidation is not completed when the amount passing the sieve is more than 40% and the vane shear strength is 0.0 kPa.

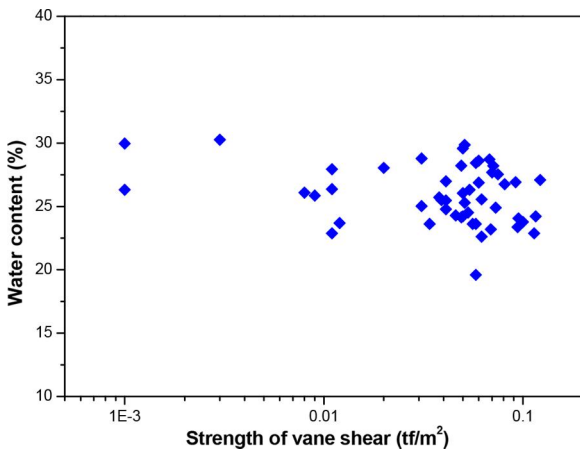


Figure 21. Relationship between vane shear strength and water content (case 1).

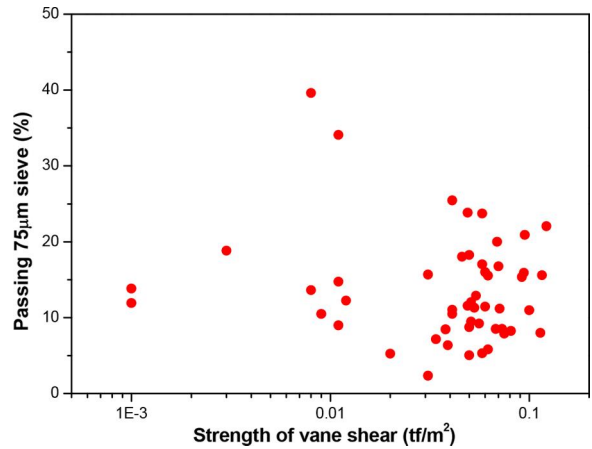


Figure 22. Relationship between vane shear strength and amount of sediment passing the 75- $\mu\text{m}$  sieve (case 1).

### Time change of pore water pressure and overburden load

Figure 23 shows the time change of earth pressure in case 1. In the figure, E1 and E2 represent earth pressure gauges. The earth pressure increases rapidly when soil is poured at each step and then decreases rapidly when the surface water is removed. The step 1 earth pressure in the observation period is almost constant, but the earth pressure in steps 2 to 4 increases as time passes. Comparing E1 to E2, the pressure is higher at E1. In other words, the earth pressure increases because the water content decreases as coarse soil settles and there is more effective soil left. Figure 24 shows the time change of pore water pressure in case 1. The piezometer installation locations are represented by P1, P2, and P3. There is almost no difference between the three locations, and the pore water pressure is almost identical with the hydrostatic pressure. Figure 25 shows the time change of the effective stress in case 1. The effective stress was calculated by subtracting the pore water pressure in Figure 24 from the earth pressure in Figure 23 (effective stress is equal to earth pressure minus pore water pressure). At E1, the maximum effective stress is 7 kPa and the final effective stress is 5 kPa. At E2, the maximum effective stress is 3 kPa and the final effective stress is 0.5 kPa.

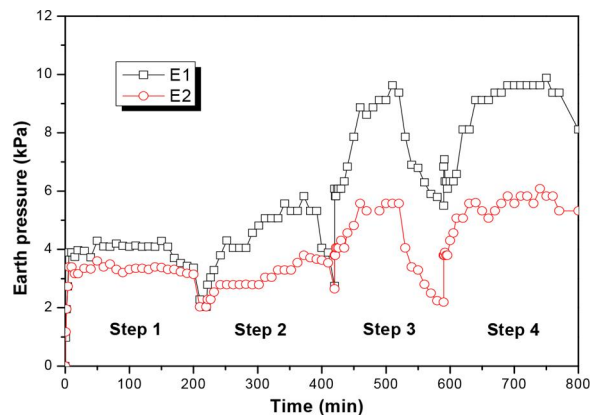


Figure 23. Time change of earth pressure (case 1).

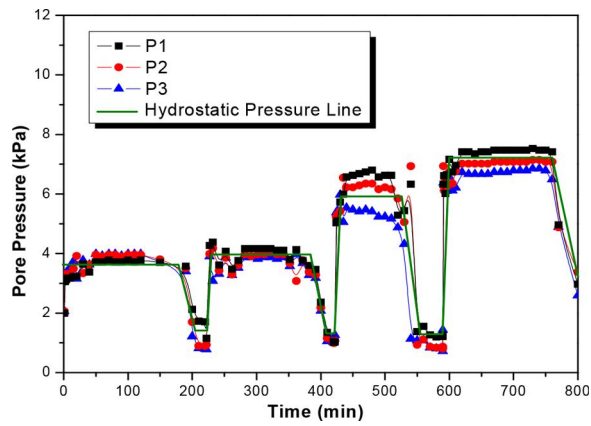


Figure 24. Time change of pore water pressure (case 1).

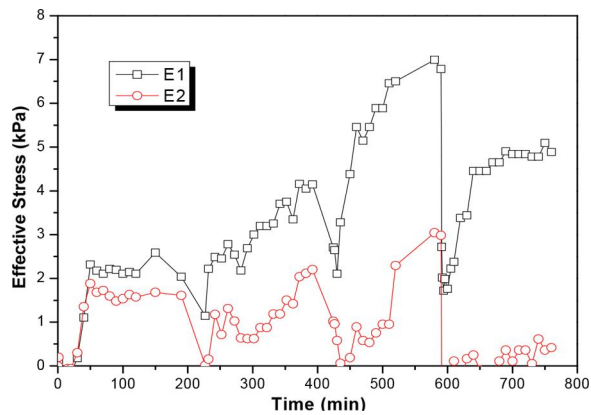


Figure 25. Time change of effective stress (case 1).

### Suggestion on outlet management method

When reclamation by pump is done on ground in contact with the surface of seawater, the physical properties and dynamics of the dredged soil are affected by its distance from the outlet. In other words, uniform reclamation of ground using the

pump reclamation method is practically impossible due to changing sedimentary conditions. Therefore, there is a high possibility of observing nonuniform settlement at the reclaimed ground. There are various methods to prevent nonuniform settlement. One of the financially favorable methods is to make the reclaimed ground uniform by changing the location of the outlet. The most suitable method is to change the location of the outlet as many times as possible, but this method is not effective because of the immense amount of time taken while changing the location of the outlet. Therefore, this research aims to suggest a possible method of changing the location of the outlet to make the reclaimed ground uniform with consideration of method constructability.

### Reclamation conditions around outlet

Figure 26 is an idealization of reclaimed ground that is being dredged. The coarse soil is mainly deposited around the outlet. Therefore, the water content is low around the outlet, and completion of self-weight consolidation is expected. On the other hand, fine soil is deposited, because of hindered settlement, in the region far from the outlet. Therefore, the water content is high and a long period of time is expected for completion of self-weight consolidation. Figure 27 shows the sedimentary conditions around the outlet. It is estimated that the poured soil is deposited conically around the outlet. If the soil height  $H$  is given, the floor diameter of the conical settlement  $D$  is calculated using Eq. (2), where  $\theta$  is the angle of the cone determined by the data from the modeling experiment. The volume of the conical deposition can be calculated using Eq. (3).

$$D = 2 \times \frac{H}{\tan \theta} \quad (2)$$

$$Q = \frac{1}{3} \times \frac{\pi D^2}{4} H \quad (3)$$

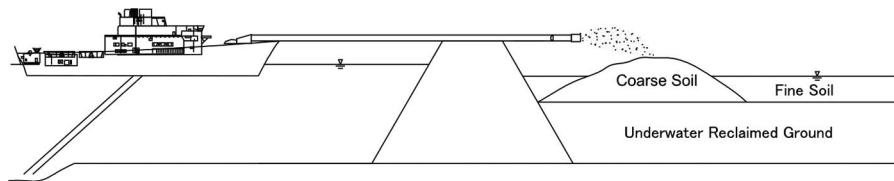


Figure 26. Idealized dredging of reclaimed ground.

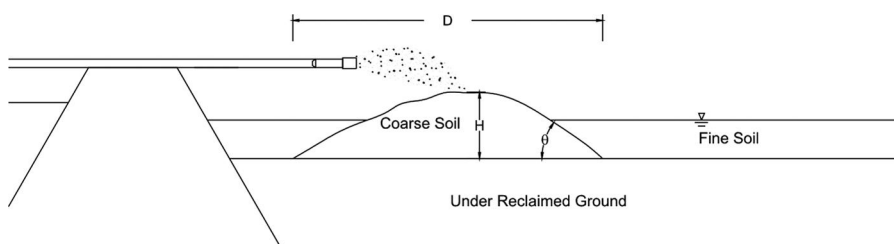


Figure 27. Sedimentary conditions around the outlet.

### Suggestion for outlet management method

When pump reclamation is used to construct reclaimed ground that is in contact with the surface of seawater, coarse soil is deposited around the outlet. On the other hand, fine soil is distributed widely throughout the reclaimed ground because its deposition is affected by hindered settling. Therefore, nonuniform reclaimed ground is formed if the location of the outlet is not controlled artificially. For uniform reclamation, the following management method is suggested:

#### Calculation of the sedimentation rate of the volume of input soil

The sedimentation rate of the volume of input dredged soil can be estimated by the modeling test. In the modeling experiment, a fixed amount of dredged soil is poured. After the input, the soil settles. By measuring the volume of the sedimentation of the soil, the sedimentation rate of the volume of the input soil can be calculated. The sedimentation rate is designated  $R_D$ .

#### Calculation of the ratio of coarse soil to total sedimentation

After completing the modeling test, collect a test sample from a portion of the deposited soil and calculate the amount of soil passing through the 75- $\mu\text{m}$  sieve. Calculate the volume of the coarse soil and the fine soil using the test results. Soil with less than 50% passage through the 75- $\mu\text{m}$  sieve is regarded as coarse soil and soil with more than 50% passage is regarded as fine soil. From the calculation, estimate the ratios of fine soil and coarse soil to total dredged soil. The ratio of the coarse soil to total dredged soil is  $C_R$ .

#### Calculation of standard coarse soil volume of sedimentation

As explained above, it is suggested that the coarse soil is deposited in a conical shape. First, calculate the volume of the conical sediment when it reaches the planned reclamation height using Eq. (3). The standard coarse soil volume of sedimentation is  $Q_b$ .

#### Overlap of coarse soil sedimentation regions

Estimate the conditions of completed reclamation using the planned reclamation height. Then determine the area of reclaimed ground by creating a square using the side dimension calculated by Eq. (2). Assume that each side of the square and the travel distance of the outlet  $L$  are identical. The volume of the determined area is calculated by the following equation:

$$Q_s = HL^2 \quad (4)$$

The volume of the cone  $Q_c$  with a bottom diameter of  $L$  is calculated by Eq. (3), and the ratio of  $Q_c$  to  $Q$ ,  $C_R$ , can be calculated by the following equation:

$$C_R = \frac{\frac{1}{3} \cdot \frac{\pi L^2}{4} H}{HL^2} = \frac{\pi}{12} \quad (5)$$

The result is the ratio of coarse soil area to the sedimentation area. In other words, the conical sediment created by

the coarse soil does not overlap other conical piles of it, if the experimental data  $C_R$  have a value less than  $\frac{\pi}{12}$ . If  $C_R$  has a value larger than  $\frac{\pi}{12}$ , the conical piles of coarse soil overlap each other.

#### Calculation of volume of input soil and travel distance of outlet when the sedimentary areas of coarse soil do not overlap

Figure 28 shows an idealization of the sedimentary conditions of the reclaimed ground when the sedimentary area of coarse soil does not include overlap. When the sedimentary area of the coarse soil does not include overlap, the top elevation of the sedimentation does not reach the planned reclamation height. In other words, the conical sedimentation gets covered by fine soil. The height of the conical sediment is  $h$ , and the volume of the sedimentation can be calculated as follows.

$$Q_C = \frac{1}{3} \times \frac{\pi L^2}{4} h \quad (6)$$

The total reclamation volume is calculated by Eq. (4). Using the  $R_D$ , calculate the volume of the input soil  $Q_P$ , as shown by the following equation:

$$Q_P = \frac{V}{R_D} = \frac{HL^2}{R_D} \quad (7)$$

Calculate the volume of the coarse soil using  $C_R$  by the following equation:

$$Q_C = Q_s \cdot C_R = HL^2 \cdot C_R \quad (8)$$

Using Eqs. (6) and (8), estimate the following equation for  $h$ .

$$h = \frac{12}{\pi} H \cdot C_R \quad (9)$$

Estimate the equation using the calculation of the travel distance of the outlet based on the geometric relationship between  $h$  and  $L$ .

$$L = 2 \times \frac{h}{\tan \theta} \quad (10)$$

#### Calculation of volume of input soil and travel distance of outlet when sedimentary area of coarse soil includes overlap

Figure 29 is an idealization of the sedimentation conditions of reclaimed ground when the sedimentation area of coarse soil includes overlaps. When the reclamation is completed, the overlap area of the conical sediment of coarse soil becomes a layered compound structure and it continues its flat overlap. Figure 30 shows the area determined by  $L$ . The coarse soil occupies the region from the bottom to the height  $h_c$ .

The volume of coarse soil in the compartmental area can be calculated by the following equation:

$$Q_C = h_c L^2 + \left( \frac{1}{3} \times \frac{\pi L^2}{4} h \right), \quad (11)$$

where  $h_c$  is the thickness of the coarse soil at the bottom of the reclaimed layer and  $h$  is the height of the conical sediment.

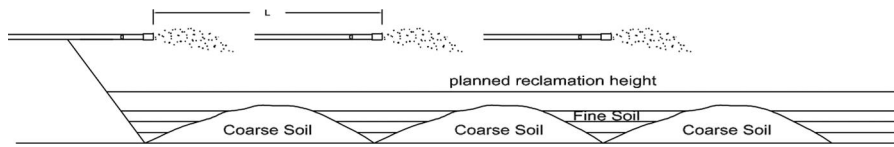


Figure 28. Idealized sedimentary conditions of reclaimed ground (no overlap).

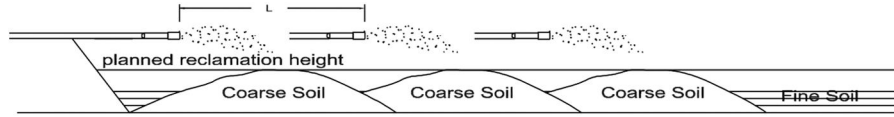


Figure 29. Idealized sedimentary conditions of reclaimed ground (with overlap).

The following equation is estimated by the geometric relationship between  $L$  and  $h$ .

$$L = 2 \times \frac{h}{\tan \theta} = 2 \times \frac{H - h_c}{\tan \theta} \quad (12)$$

The next equation is then established by the calculation of Eq. (12).

$$h_c = H - \frac{1}{2}L \tan \theta \quad (13)$$

By substituting Eq. (13) into Eq. (11), the following equation is established.

$$Q_C = \left( H - \frac{1}{2}L \tan \theta \right) \times L^2 + \left( \frac{1}{3} \times \frac{\pi L^2}{4} \times \frac{1}{2}L \tan \theta \right) \quad (14)$$

The volume of the coarse soil is calculated by Eq. (8). Then, the equation below is established by Eqs. (8) and (14).

$$HL^2 \cdot C_R = \left( H - \frac{1}{2}L \tan \theta \right) \times L^2 + \left( \frac{1}{3} \times \frac{\pi L^2}{4} \times \frac{1}{2}L \tan \theta \right) \quad (15)$$

Finally, the following equation is established by the calculation of  $L$  from Eq. (15).

$$L = \frac{24 \cdot (C_R - 1)H}{(\pi - 12) \tan \theta} \quad (16)$$

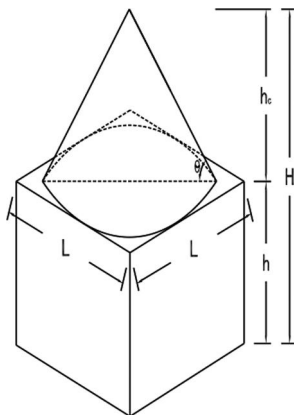


Figure 30. Area determined by  $L$ .

In addition, the volume of the input soil can be calculated using Eq. (7).

### Trial calculation of outlet management method

Using the modeling test data, calculate the travel distance of the outlet  $L$  and the volume of the input soil  $Q_p$ . Assume that the planned reclamation height is 10 m and that the reclamation of cases 1 and 2 will use coarse soil.

### Calculation of sedimentation rate to volume of input soil

Table 5 shows the rate of sedimentation to the volume of the input soil for the modeling test. In the test, 0.63 m<sup>3</sup> dredged soils with 700% water content were divided and poured in four different stages. Therefore, the total input volume of the soil is 2.52 m<sup>3</sup>. In addition, the volume of the sedimentation for case 1 and 2 was 0.65 and 0.69 m<sup>3</sup>, respectively. The rate (ratio) of the sedimentation to the volume of the input soil is 0.258 for case 1 and 0.274 for case 2.

### Calculation of rate of coarse soil to volume of sedimentation

Table 6 shows the rate of coarse soil to the volume of sedimentation in the modeling test. The rate of the volume of coarse soil to the volume of the sedimentation,  $C_R$ , is 0.54 for case 1 and 0.07 for case 2.

Table 5. Rate of sedimentation to volume of input soil.

Case	Volume of input soil (m <sup>3</sup> )	Sedimentation	
		Volume (m <sup>3</sup> )	Rate, $R_D$
1	2.52	0.65	0.258
2	2.52	0.69	0.274

Table 6. Rate of coarse soil to volume of sedimentation.

Case	Sedimentation		
	Total Volume (m <sup>3</sup> )	Coarse soil Volume (m <sup>3</sup> )	Rate, $C_R$
1	0.65	0.35	0.54
2	0.69	0.05	0.07

### Calculation of standard coarse soil volume of sedimentation

Table 7 shows the standard coarse soil volume of sedimentation. The angle of the slope in case 1 is  $23^\circ$  and that in case 2 is  $19^\circ$ . The volume of standard coarse soil sedimentation,  $Q_b$ , was estimated by the calculation of  $H$  and  $D$  using Eqs. (2) and (3).

### Overlap of coarse soil sedimentation regions

Table 8 shows the overlap results of the sedimentation area. Estimate the overlap of the conical sediment of the coarse soil by the zone ratio to  $\frac{\pi}{12}$ . Case 1 has a coarse soil zone ratio that is larger than the value of  $\frac{\pi}{12}$ , and the sediment caused by the coarse soil overlaps. However, case 2 has a coarse soil zone ratio that is smaller than the value of  $\frac{\pi}{12}$ , and the conical sediment of coarse soil does not overlap.

### Calculation of volume of input soil and travel distance of outlet when sedimentary area of coarse soil does not overlap

Table 9 shows the travel distance of the outlet and the volume of the input soil. First, calculate the conical sediment height using Eq. (9). Then, calculate the travel distance of the outlet,  $L$ , using Eq. (10). As a result,  $L$  is equal to 15.5 m. The volume of the input soil is calculated using Eq. (7), and its value is  $8768 \text{ m}^3$ . In other words, the outlet travels 15.5 m, and the volume of dredged soil is  $8,763 \text{ m}^3$ .

### Calculation of the volume of the input soil and the travel distance of the outlet when the sedimentary area of the coarse soil overlaps

Table 10 shows the travel distance of the outlet and the volume of the input soil when the sedimentation areas overlap. First, calculate the travel distance of the outlet using Eq. (17). As a result,  $L$  is equal to 29.4 m. Next, calculate the volume of the input soil at location using Eq. (7). The

**Table 7.** Standard coarse soil volume of sedimentation.

Case	Amount passing 75- $\mu\text{m}$ sieve (%)	$\theta$ ( $^\circ$ )	$\tan \theta$	$H$ (m)	$D$ (m)	$Q_b$ ( $\text{m}^3$ )
1	20	23	0.424	10	47	5783
2	45	19	0.344	10	58	8807

**Table 8.** Overlap results of the sedimentation area.

Case	Amount passing 75- $\mu\text{m}$ sieve (%)	Coarse soil zone ratio, $C_R$	Criterion, $C_R$	Note
1	20	0.54	$\frac{\pi}{12} \approx 0.262$	Overlap
2	45	0.07		No overlap

**Table 9.** Travel distance of outlet and the volume of the input soil when sedimentation areas do not overlap.

Amount passing 75- $\mu\text{m}$ sieve (%)	$h$ (m)	$L$ (m)	$Q_c$ ( $\text{m}^3$ )	$Q_p$ ( $\text{m}^3$ )
45	2.7	15.5	168	8768

**Table 10.** Travel distance of outlet and volume of input soil when sedimentation areas overlap.

Amount passing 75- $\mu\text{m}$ sieve (%)	$L$ (m)	$h_c$ (m)	$Q_c$ ( $\text{m}^3$ )	$Q_p$ ( $\text{m}^3$ )
20	29.4	3.8	4667	33502

volume is equal to  $33,502 \text{ m}^3$ . In other words, the poured volume of dredged soil is  $33,502 \text{ m}^3$ , and the travel distance of the outlet is 29.4 m.

### Conclusion

This study demonstrates a modeling test to understand the characteristics of new sedimentary ground using the changing ratio of two types of samples passing the 75- $\mu\text{m}$  sieve. From the test results, the research determined the effect of particle arrangement on hindered settling properties, sedimentation properties, the distribution of water content of sedimentary ground, and physical properties. Additionally, the research suggested the calculation method for the travel distance of the outlet and the volume of the input soil based on the experimental data. The following conclusions can be drawn on the basis of results of the experiment:

### Characteristics of sedimentation based on experiments

- (1) Segregation of sedimentation takes place near the outlet right after the moment of input of the dredged soil. After that, hindered settling is observed. Most of the fine soil is transferred far from the outlet by the pressure of the pump, floating horizontally. The fine soil is eventually deposited despite the hindered settling.
- (2) The velocity of the hindered settling is faster and the volume of self-weight consolidation is lower near the outlet.
- (3) The stable angle of the dredged soil's slope allows the coarse soil sediment to independently maintain itself, and the angle of the slope increases as a larger amount of coarse soil is included in the soil.
- (4) The water content of the sedimentary ground near the outlet is low owing to the sedimentation of coarse soil. However, in the area far from the outlet, the water content of the ground is high due to sedimentation of fine soil in the region.
- (5) The rate of the amount of soil in the dredged soil passing the 75- $\mu\text{m}$  sieve increases with distance from the outlet. When using the dredged soil sample with a 20% fraction passing the sieve, the sediment at distance from the outlet is mixed and disturbed by poured soil and demonstrates hindered settling. Therefore, the rate of soil passing the sieve increases with proximity to the surface. On the other hand, when the dredged soil sample with a 40% fraction passing the sieve was used, the fine soil became mixed and disturbed at a distance from the outlet, and a vertical distribution was not distinguished. Therefore, the distribution of the particles in the fine soil sedimentation area and the vertical profile is affected by the particle arrangement.

### Suggestion for outlet management method

- (6) In the experiment using the dredged soil with a 20% fraction passing the 75- $\mu\text{m}$  sieve, the fine soil sedimentation ratio to the total sediment was 46.4%. Therefore, it is suggested that the ratio of fine soil to total reclamation ground is significant, even if the dredged soil includes a fair amount of the coarse soil.
- (7) Irrespective of the rate of coarse soil, the water content of the sediment increases proportionally to the fraction passing the 75- $\mu\text{m}$  sieve until it reaches 80%.
- (8) Vane shear strength is observed mostly at sites where coarse soil is deposited.
- (9) A thicker sedimentary layer of coarse soil is observed near the outlet; therefore, the effective stress of the coarse soil is larger than that in the area of fine-soil sedimentation.
- (10) When constructing reclaimed ground, the travel distance of the outlet and the volume of input soil can be adjusted according to the sedimentary conditions of the coarse soil and fine soil.

### ORCID

Min-Sun Lee  <http://orcid.org/0000-0002-9811-8618>

### References

- Chu, J., M. W. Bo, and A. Arulrajah. 2009. Reclamation of a slurry pond in Singapore. *Proc the Institution of Civil Engineers (UK), Geotechnical Engineering* 162 (1):13–20. doi:10.1680/geng.2009.162.1.13.
- Ghazavi, M., M. Hosseini, and M. Mollanouri. 2008. A comparison between angle of repose and friction angle of sand. The 12th International Conference of International Association for Computer Methods and Advances in Geomechanics, IACMAG, 1272–1275.
- Hough, B. K. 1957. *Basic soils engineering*. New York: The Ronald Press Company.
- Imai, G. 1980. Settling behavior of clay suspension. *Soils and Foundations* 19 (3):45–60. doi:10.3208/sandf1972.20.2\_61.
- Imai, G. 1981. Experimental studies on sedimentation mechanism and sediment formation of clay materials. *Soils and Foundations* 21 (1):7–20. doi:10.3208/sandf1972.21.7.
- Lee, M. S., and K. Oda. 2013a. Evaluation of post-surcharge secondary settlement characteristics by constant rate of strain test. *Geotechnical Testing Journal, ASTM* 36 (3):1–7. doi:10.1520/gtj20120049.
- Lee, M. S., and K. Oda. 2013b. Evaluating self-weight consolidation for dredged soil mixed with coarse-grained soils. *International Journal of Offshore and Polar Engineering, IJOPE* 23 (4):307–312.
- Lee, M. S., and K. Oda. 2015. Evaluation of excess pore water pressure characteristics in sand mat used for recycling dredged soil. *Marine Georesources & Geotechnology* 33 (5):367–375. doi:10.1080/1064119x.2014.890985.
- Masaaki, K., T. Masaaki, and K. Akira. 2001. Back analysis of reclamation by pump-dredged marine clay—influence of ground water lowering. *Soils and Foundations* 41 (5):73–86. doi:10.3208/sandf.41.5\_73.